Hybrid Angiosperm Root Systems Structural Analysis Using Convolutional Neural Network

Jose Miguel F. Custodio[1], Ronnie Concepcion II[1,2], Renann Baldovino[1,2], Ryan Rhay Vicerra[1,2], Luigi Gennaro Izzo[3]
[1]*Department of Manufacturing Engineering and Management, De La Salle University,* Manila, Philippines
[2]*Center for Engineering and Sustainability Development Research, De La Salle University,* Manila, Philippines
[3]*Department of Agricultural Sciences, University of Naples Federico II,* Portici, Italy
{jose_miguel_f_custodio, ronnie.concepcion, renann.baldovino, ryan.vicerra}@dlsu.edu.ph, luigigennaro.izzo@unina.it

***Abstract*—Analysis of root images is a significant part of root studies for gathering data on key traits of root systems. Better understanding of plant roots and its interactions are beneficial to the agricultural sector. These allow for better designing of cultivation systems and techniques that optimize the resource use efficiency of crops. Studying root structures may entail the use of imaging methods and further image analysis. Here, the use of convolutional neural network (CNN) is explored as tool to classify root images as monocot (banana, corn) or dicot (peas, peach, germander, pennycress) plants and to extract the numerical value of total root length as the main crop phene. The results of the ReLU-activated PriceNet CNN classification model showed a high accuracy of 99.2% in sorting images as monocot or dicot. The PriceNet regression model for total root length exhibited an R^2 value of 0.903 and it was able to perform the analysis without separating monocot and dicot image datasets. These models were also able to speedily perform test predictions, requiring 4-5 seconds to process the 1500 test samples. This confirms the fast computation potential that neural networks have in image analysis. As an additional benefit, the regression model was trained to predict total root length for both monocot and dicot root systems and work with datasets with mixed compositions of images.**

Keywords*—*Convolutional Neural Network, Root Imaging, Classification, Regression, Feature Extraction

I. Introduction

Plant roots are underground organs mainly responsible for absorbing water and nutrients from the soil. Because of this role, advancements in root studies would help improve plant productivity and in turn, improve agricultural yields and food security [1]. Some innovations include creating zones of high nutrient density to maximize the crop yields while lessening the total amount of nutrients needed in soil preparation [2]. Analysis of root traits is also a method explored in assessing plant health and detecting disease, such as the use of dataset analysis to quantify damages to cassava root caused by necrosis [3].

One basic aspect in root analysis refers to the classifications that flowering plants fall under, monocot and dicot [4]. The divergence of the two families is largely shown through morphological differences, such as the shape and venation of leaves and the structure of roots [5]. Dicot roots are identified to be generally taproot systems with single primary roots, whereas monocots have fibrous root systems with multiple primary roots. These differences also affect root features such as lateral root growth and how vascular tissues are organized in the roots [6]. These variations also lead to differences in function, as dicot/monocot crop rotations have been observed to benefit the diversity of beneficial microorganisms in soil, suggesting better soil fertility [7]. For root imaging, to allow for proper characterization, root analysis schemes should be able to discern between dicot and monocot root structures.

In the field of plant root imaging, rhizotron setups are valuable tools to study root systems. These are planting containers which use transparent material as windows through which the roots of the plant can be seen as it grows through soil or other media. This overcomes the initial barriers to studying roots, the opaque nature of the surrounding soil. The design of their dimensions also constrains the growth of the roots to be relatively flat or two dimensional to easily image the entire root system [8]. Medical imaging techniques such as MRI and X-ray CT scans have been developed to also allow for 3D root imaging [8], [9]. Electrical tomography methods have also been explored for this purpose [10].

Previously, to obtain data from rhizotron setups, manual tracing was required [11]. This method can be time consuming and inaccurate due to human error and inaccuracies. Scanners and cameras suited for the task have been developed help minimize error during data collection. These are then fed to specially developed algorithms and software to digitally extract data from the acquired root images. One such successful method among others is the WinRHIZO software, a flexible software for root analysis [12]. Other root architecture analysis programs include MyROOT, RhizoChamber-Monitor, and ARIA [13]–[15]. There also exist software dedicated to simulating synthetic root systems under different conditions, such as OpenSimRoot [16]. These various tools help better understand root architectures for improving agricultural yields and ensuring plant health.

The trending interest with neural networks and other machine learning methods was brought about by the increase in computer processing power [17]. Convolutional neural network (CNN) has successfully been used in different fields for the purpose of image analysis to predict data. These include price prediction, inversion algorithm, and Covid detection [18]–[20]. The versatility of neural networks come from the design of their architecture, with larger and deeper designs being capable of learning more complex features [21]. As an example, the ChronoRoot system combines 3D printed rhizotron setups with CNNs for the purpose of time-based root image studies [22]. When utilized for root analysis, it allows the development of feature extraction systems with minimal supervision, rather than developing specialized algorithms for each desired measurement. Neural networks also have the benefit of having fast prediction speeds after the computationally heavy training period [23].

Aside from CNN, other machine learning techniques have been used for root architecture and adjacent studies. The MyROOT software utilizes support vector machine models to differentiate the hypocotyls and roots of seedlings [13]. Random forest, artificial neural network, and support vector machine techniques have been used to classify plants to different levels of root-soil moisture based on phenotyping traits, to aid in precision irrigation systems [24].

For the objectives of image analysis of this study, PriceNet, an existing CNN architecture, will be used. PriceNet was initially developed to derive price ranges and exact price values of commercially available bikes and vehicles from singular images [18]. This architecture was selected due to its

TENCON 2022 - 2022 IEEE Region 10 Conference (TENCON) | 978-1-6654-5095-9/22/$31.00 ©2022 IEEE | DOI: 10.1109/TENCON55691.2022.9977873

relative simplicity and capability to be used on both regression and classification problems just with adjustments to the output layers [18]. In addition, overly complex models for a task can run the risk of having redundant parameters and overfit to the training data [21].

To aid in understanding root architectures, this study aims to explore the utilization of convolutional neural networks, particularly PriceNet, for the study and analysis of root images. The identification of functional CNN models would help provide another tool in crop root studies and demonstrate the versatility of neural networks. The target output of the neural network is the categorization of monocot and dicot species and the extraction of data on total root length of the imaged root systems. The study utilizes available synthetic image libraries for the training of the CNN.

II. Methodology

The processes of the methodology can be summarized in Fig. 1 below. The first two steps prepare the dataset for the CNN to use. The images that will be taken as input will be resized to similar sizes, while the output values are compiled onto a csv file. The training of the CNNs will then be executed through TensorFlow and Keras, during which, epochs with the best performing models are saved. These saved models are then tested and evaluated. Finally, the developed PriceNet models will be compared to the previous study's performance.

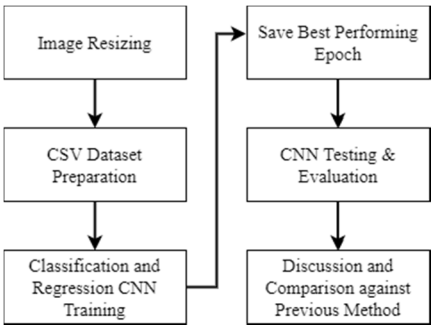

Fig. 1. Methodological architecture in classifying monocot and dicot species and regressing root length based on imaged root systems using CNN.

A. Description of Root Image Dataset

The dataset utilized in the study is acquired from a previous study that generated the dataset for the purpose of assisting root research studies [25]. It comprises three components: 10,000 images, true descriptor csv files, and estimator csv files. The images were simulated greyscale figures synthesized by ArchiSimple, a root model program, with a 50%:50% split between monocot and dicot root systems. ArchiSimple was created to generate root systems based on physiological parameters [26]. By basing the growth patterns of the roots primarily on physiological parameters such as root diameters, it allows the program to become independent from predetermined root categories and species. This is unlike other root modeling programs that are based on growth patterns of specific plants. By adjusting these generic parameters, ArchiSimple can then be calibrated to emulate root systems that are characteristic of specific species [26]. Each image was created with randomly generated values for the physiological parameters, thus are not necessarily representatives of specific plant species. The simulated plant roots were constrained to only grow in a 2D space.

The second part of the dataset are values directly obtained from the ArchiSimple and are true descriptors for the images. The morphological and geometric traits of the model were: total root length, total primary root length, total lateral root length, mean of primary root lengths, mean of lateral root lengths, number of primary roots, number of lateral roots, density of lateral roots, mean diameter of primary roots, mean diameter of lateral roots, and insertion angle of lateral roots [25]. The parameter values used to generate each image are then compiled to a csv file. Some of the images from the dataset are shown in Fig. 2. Labels were added to the figure to point out the surface level, lateral roots, and primary roots of the figures. These parts of the root system hold different purposes for the overall root architecture [27].

B. Description of Root Estimators Dataset

The third portion of the dataset, the estimator csv files, utilized Root Image Analysis-J (RIA-J), a plugin for image analysis, to generate descriptive estimator traits from the synthetic root images. The estimators include root area, length, root tip count, mean diameter of roots, maximum width and depth, width-depth ratio, center of mass coordinates, area of minimal convex shape, and convex area-root area ratio [28].

The dataset's developers then proceeded to train random tree networks to relate these estimators to the actual true parameters of the images. This was done to test the potential of synthetic analysis for the study of root data. The developers trained these networks separately for monocot and dicot data, after they concluded that there are significant differences between the values of the two root systems.

The CNN models in the next two sections will attempt to use the dataset of both monocot and dicot roots simultaneously, both to classify between the two types and to predict total root lengths of both root systems. When compiled, the 10,000 values for total root length have a range of 6.911 to 2,455.025 mm.

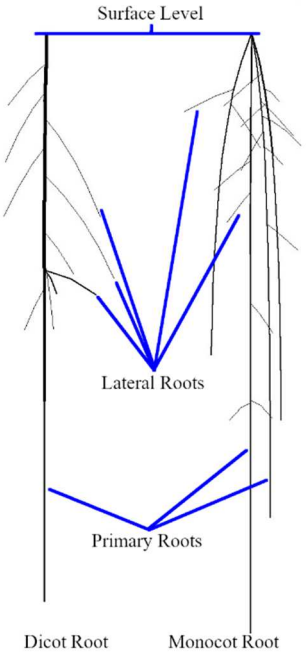

Fig. 2. Sample images from the Simulated Root Images Library [25].

The images generated had variable dimensions, with widths ranging from 130 to 4023 pixels and heights ranging from 1221 to 5001 pixels. To both reduce the size and present uniformity to the image sizes, the images were all resized to a 300 x 400 resolution. This was done through batch processing features in GNU Image Manipulation Program (GIMP) 2, an

open-source image editor. The selected resolution was arbitrarily selected, with a longer height due to the elongated nature of the original images.

C. Classification Modeling Using PriceNet

Due to the two desired outputs of this study, two CNN models were trained from the same architecture. The first is a classification model to determine if images are from monocot or dicot plants. The second is a regression model that would predict the total root length of the root system.

The CNN architecture used is PriceNet. The layers of this architecture can be seen below in table 1, along with their output shape. PriceNet features four pairs of convolution and max pooling layers. The data is then flattened and followed by two dense layers. Rectilinear Unit (ReLU) activations are added between each convolution and pooling layer. For the classification model, a sigmoid activation layer is placed at the end of the final dense layer.

TABLE 1. CNN ARCHITECTURE LAYERS OF PRICENET

Layer	Output Shape
2D Convolution (32, 5x5)	(None, 400, 300, 1)
Max Pooling 2D (2x2)	(None, 400, 300, 32)
2D Convolution (64, 5x5)	(None, 200, 150, 32)
Max Pooling 2D (2x2)	(None, 200, 150, 64)
2D Convolution (64, 5x5)	(None, 100, 75, 64)
Max Pooling 2D (2x2)	(None, 50, 37, 64)
2D Convolution (128, 5x5)	(None, 50, 37, 128)
Max Pooling 2D (4x4)	(None, 12, 9, 128)
Flatten	(None, 13824)
Dense (512)	(None, 512)
Dense (1)	(None, 1)

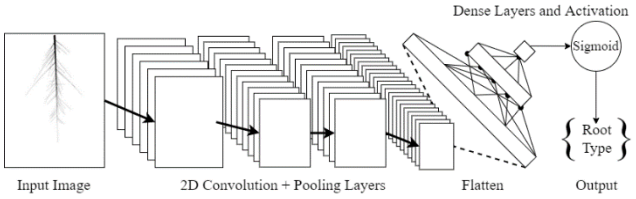

Fig. 3. Configured PriceNet deep learning architecture for angiosperms classification as monocotyledon or dicotyledon with root system images as inputs.

The models were initialized and trained through the Keras 2.9.0 and Tensorflow 2.3.0 libraries of Python. The processing was performed on a desktop computer with a Ryzen 5 3500x CPU (6 Cores @ 3.6 GHz) and 16 GB of RAM. The installation of NVIDIA's CUDA and CuDNN packages enabled Tensorflow to utilize the GTX 1060 GPU of the desktop computer, speeding up the model training step significantly.

The monocot and dicot images and data were compiled into a singular dataset and split with a 70%:15%:15% ratio for training, validation, and testing each of the two models. Each are developed independently from each other. The classification model was trained for five epochs with a learning rate of 0.001.

D. Root Length Regression Modeling Using PriceNet

The CNN used for the root length regression model was also PriceNet, with the same layer and architecture design shown in TABLE 1. It has been configured for regression, by activating the final dense layer with a ReLU function instead of the sigmoid function used in the classification model. This allows the output to be any positive real number.

The regression model was trained for 30 epochs and a learning rate of 0.00001. The best model generated across the 30 epochs, in terms of mean squared error (MSE), was saved. This saved model was evaluated for testing, which had used 15% of the dataset to assess the performance of the models on the untrained data.

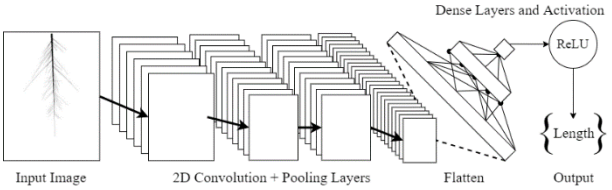

Fig. 4. Configured PriceNet deep learning architecture for root length regression with root system images as inputs.

E. Model Evaluation Metric

The configured classification CNN model was evaluated using accuracy, fall-out, precision, specificity, recall, f1-score, Matthew's correlation coefficient (MCC), and Hamming loss that were derived from the corresponding confusion matrix. The true positive (TP) in this case would refer to images correctly labelled as monocot root systems, while true negatives (TN) refer to images correctly labelled as dicots.

$$Accuracy = \frac{TP+TN}{TP+FP+TN+FN} \quad (1)$$

$$Fall-out = \frac{FP}{FP+TN} \quad (2)$$

$$Precision = \frac{TP}{TP+FP} \quad (3)$$

$$Specificity = \frac{TN}{FP+FN} \quad (4)$$

$$Recall = \frac{TP}{TP+FN} \quad (5)$$

$$F1-Score = \frac{2TP}{2TP+FP+FN} \quad (6)$$

$$MCC = \frac{TP*TN-FP*FN}{\sqrt{(TP+FP)(TP+FN)(TN+FP)(TN+FN)}} \quad (7)$$

$$Hamming\ Loss = \frac{FP+FN}{TP+FP+TN+FN} \quad (8)$$

On the other hand, the regression CNN model was evaluated on MSE, coefficient of determination (R^2), and mean absolute error (MAE) as the selected metrics to evaluate the error of its predictions and its overall accuracy.

$$MSE = \frac{1}{n}\sum(True\ Value - Predicted\ Value)^2 \quad (9)$$

$$R^2 = 1 - \frac{\sum(True\ Value-Predicted\ Value)^2}{\sum(True\ Value-Average\ True\ Value)^2} \quad (10)$$

$$MAE = \frac{1}{n}\sum|True\ Value - Predicted\ Value| \quad (11)$$

III. RESULTS AND DISCUSSION

A. Sensitivity of PriceNet in Classifying Angiosperms

The saved classification model has a size of 56.8 MB and required a training time of 37.6 minutes. To sort the 1500 test images, the classification model has a total run time of 4.06

seconds or an average of 0.00271 seconds per image. The results of the 1500 test predictions are summarized in the confusion matrix, shown in Fig. 5 below. There is a total of 1,488 predictions that matched the true root system of the image, and 12 inaccurate predictions, which come from six dicot and six monocot root systems falsely predicted as the other. Overall, the model achieved a total accuracy of 99.2%. The other metrics are summarized in TABLE 2, displaying high values for precision, specificity, recall, f1-score, and Matthew's correlation coefficient. On the other hand, the fall-out and hamming loss have small values, indicating low false positive rates. These metrics suggest that the model is highly capable at distinguishing the two root systems from each other, with little error.

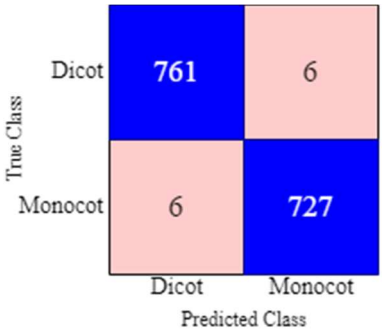

Fig. 5. Confusion matrix of classification model predictions.

TABLE 2. SUMMARY OF EVALUATION METRICS FOR THE CLASSIFICATION PRICENET MODEL

Classification Metric	Test Value
Accuracy (%)	99.200
Fall-Out (%)	0.782
Precision (%)	99.181
Specificity (%)	99.218
Recall (%)	99.181
F1-Score (%)	99.181
MCC (%)	98.399
Hamming loss (%)	0.800

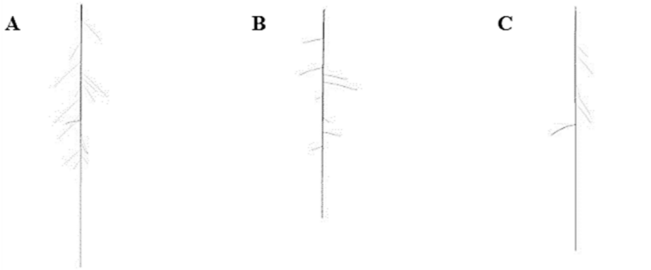

Fig. 6. Sample test images with true and predicted root type.

The model was not perfect and Fig. 6 shows three similar root images, two of which (B and C) were mislabeled by the classification model. Among the various architectures captured by root images, the ones portrayed in Fig. 6 are similarly characterized by a straight primary root with a sparse number of lateral roots. This form of root system having representatives in both monocot and dicot may explain why the CNN model was unable to perfectly predict the root category of all images. Even so, the model was able to accurately predict images with this root architecture variant, such as the case of Figure 6A correctly tagged as dicot.

B. Sensitivity of PriceNet in Regressing Root Length

As for the trained regression model, it had a larger size of 85.1 MB and finished its training in 23.6 minutes. In terms of prediction speed, the regression model was slightly slower, requiring 5.02 seconds for the entire test of 1500 images or 0.00335 seconds for each image. Fig. 7 shows the model's predicted values for 150 samples, showing good fitting to the dataset's true values. This is despite the large range of true values, ranging from 10^0 to 10^3 in magnitude.

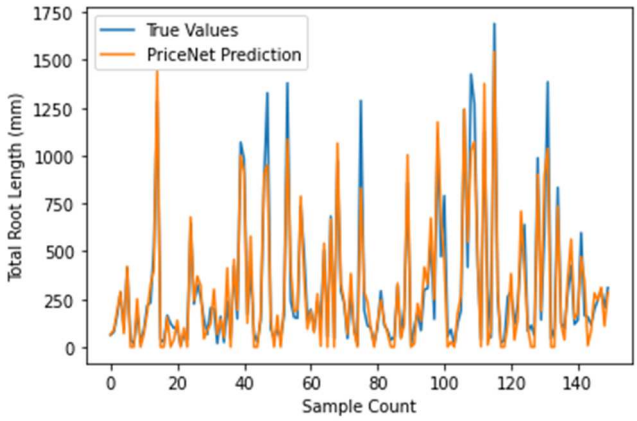

Fig. 7. Comparison between PriceNet total root length predictions and the true expected values.

The evaluation metrics acquired, as shown in TABLE 3, shows that the model achieved an R^2 of 0.905 for the 1500 test images, without having to train the model separately for monocot and dicot root data. This is a sufficiently accurate model. To compare, the initial purpose of PriceNet for predicting bike prices achieved an R^2 of 0.85 [18]. In addition to these, the trained model's MSE has a value of 10920.336 mm and an MAE of 72.397 mm. These high error values may be attributed to the extreme high and low lengths present in the dataset. In comparison, the length estimator found in the dataset was less accurate than developed PriceNet model, with only an R^2 score of 0.758 and higher MSE and MAE values.

TABLE 3. SUMMARY OF EVALUATION METRICS FOR THE PRICENET REGRESSION MODEL AND RIA-J ESTIMATOR VALUES

Regression Metric	PriceNet Regression Model	RIA-J Estimated Length
MSE (mm^2)	10920.336	27928.676
R^2 score (-)	0.905	0.758
MAE (mm)	72.397	83.18

In addition to the two models, an attempt was made to utilize the regression architecture on other root traits such as lateral angle and tip count, but these did not develop accurate models. It can be surmised that a more sophisticated CNN architecture is necessary to be able to create accurate root extraction models for more root traits beyond just total root length.

This single process method is simpler in comparison to the original study's method, which utilized two steps to predicting root values: Use RIA-J to create descriptors, then pass these descriptors to the random tree algorithm to generate the predictive model. The research also trained the algorithms separately for dicot and monocot data, due to the distinct

differences in their root architectures [25]. This proposed method of training CNN models, however, aimed to utilize one step by directly predicting root trait values from the images. Should an appropriate architecture be developed, this would streamline the process of prediction and be able to work with both dicot and monocot root systems simultaneously.

IV. Conclusion

As the demand for food productivity would increase over the years, maximizing the yields from each crop becomes an important matter for food security. Root studies are one of the avenues available that can improve crop yields by enhancing the capability of plants to absorb water and nutrients from the surrounding soil. Due to the opacity of soil, these studies rely on imaging techniques and data processing to extract information from 2D or 3D root images. To assist in root image interpretation and analysis, this study presented the use of CNN for the purpose of monocot-dicot classification and total root length regression. By utilizing the PriceNet architecture, the created classification and regression models were able to perform their tasks with high accuracy and evaluation metrics. The speed offered by the model is a major benefit of neural networks once trained, requiring only 4-5 seconds to predict the 1500 test images.

Further comparison of CNN models with other architectures in terms of speed and size would also provide important information on the tradeoffs of using different techniques. This is especially true when developing systems with constraints in processing power and memory.

Acknowledgment

The authors would like to thank the Philippines' Department of Science and Technology-Engineering Research and Development for Technology (DOST-ERDT), the Office of Vice President in Research and Innovation and the Intelligence Systems Laboratory of the De La Salle University, Manila, for all the granted supports.

References

[1] P. F. Zhao *et al.*, "Electrical imaging of plant root zone: A review," *Computers and Electronics in Agriculture*, vol. 167, no. September, p. 105058, 2019, doi: 10.1016/j.compag.2019.105058.

[2] J. Jing *et al.*, "Harnessing root-foraging capacity to improve nutrient-use efficiency for sustainable maize production," *Field Crops Research*, vol. 279, no. September 2021, p. 108462, 2022, doi: 10.1016/j.fcr.2022.108462.

[3] J. Nakatumba-Nabende, B. Akera, J. F. Tusubira, S. Nsumba, and E. Mwebaze, "A dataset of necrotized cassava root cross-section images," *Data in Brief*, vol. 32, Aug. 2020, doi: 10.17632/gvp7vshvnh.3.

[4] Q. Liu *et al.*, "Transcriptional landscape of rice roots at the single-cell resolution," *Molecular Plant*, vol. 14, no. 3, pp. 384–394, Mar. 2021, doi: 10.1016/j.molp.2020.12.014.

[5] H. Nelissen, N. Gonzalez, and D. Inzé, "Leaf growth in dicots and monocots: So different yet so alike," *Current Opinion in Plant Biology*, vol. 33. Elsevier Ltd, pp. 72–76, Oct. 01, 2016. doi: 10.1016/j.pbi.2016.06.009.

[6] Y. Chen *et al.*, "A comparison of lateral root patterning among dicot and monocot plants," *Plant Science*, vol. 274, pp. 201–211, Sep. 2018, doi: 10.1016/j.plantsci.2018.05.018.

[7] A. G. Albarracín Orio, E. Brücher, and D. A. Ducasse, "Switching between monocot and dicot crops in rotation schemes of Argentinean productive fields results in an increment of arbuscular mycorrhizal fungi diversity," *Applied Soil Ecology*, vol. 98, pp. 121–131, Feb. 2016, doi: 10.1016/j.apsoil.2015.10.004.

[8] J. A. Atkinson, M. P. Pound, M. J. Bennett, and D. M. Wells, "Uncovering the hidden half of plants using new advances in root phenotyping," *Current Opinion in Biotechnology*, vol. 55. Elsevier Ltd, pp. 1–8, Feb. 01, 2019. doi: 10.1016/j.copbio.2018.06.002.

[9] L. G. Izzo, L. E. Romano, S. de Pascale, G. Mele, L. Gargiulo, and G. Aronne, "Chemotropic vs Hydrotropic Stimuli for Root Growth Orientation in Microgravity," *Frontiers in Plant Science*, vol. 10, Nov. 2019, doi: 10.3389/fpls.2019.01547.

[10] D. D. J. C. Lopez, S. Sommer, S. A. Rolfe, F. Podd, and B. D. Grieve, "Electrical impedance tomography as a tool for phenotyping plant roots," *Plant Methods*, pp. 1–15, 2019, doi: 10.1186/s13007-019-0438-4.

[11] A. Mohamed *et al.*, "An evaluation of inexpensive methods for root image acquisition when using rhizotrons," *Plant Methods*, vol. 13, no. 1, Mar. 2017, doi: 10.1186/s13007-017-0160-z.

[12] F. HUI *et al.*, "Image-based root phenotyping for field-grown crops: An example under maize/soybean intercropping," *Journal of Integrative Agriculture*, vol. 21, no. 6, pp. 1606–1619, Jun. 2022, doi: 10.1016/S2095-3119(20)63571-7.

[13] I. Betegón-Putze, A. González, X. Sevillano, D. Blasco-Escámez, and A. I. Caño-Delgado, "MyROOT: a method and software for the semiautomatic measurement of primary root length in Arabidopsis seedlings," *Plant Journal*, vol. 98, no. 6, pp. 1145–1156, Jun. 2019, doi: 10.1111/tpj.14297.

[14] J. Wu *et al.*, "RhizoChamber-Monitor: A robotic platform and software enabling characterization of root growth," *Plant Methods*, vol. 14, no. 1, Jun. 2018, doi: 10.1186/s13007-018-0316-5.

[15] J. Pace, N. Lee, H. S. Naik, B. Ganapathysubramanian, and T. Lübberstedt, "Analysis of maize (Zea maysL.) seedling roots with the high-throughput image analysis tool ARIA(Automatic root image analysis)," *PLoS ONE*, vol. 9, no. 9, Sep. 2014, doi: 10.1371/journal.pone.0108255.

[16] J. A. Postma *et al.*, "OpenSimRoot: widening the scope and application of root architectural models," *New Phytologist*, vol. 215, no. 3, pp. 1274–1286, Aug. 2017, doi: 10.1111/nph.14641.

[17] M. Vu and H. Sciences, "Convolutional neural networks with SegNet architecture applied to three- dimensional tomography of subsurface electrical resistivity. CNN-3D-ERT," no. January, 2021, doi: 10.1093/gji/ggab024.

[18] S. Chen, E. Chou, and R. Yang, "The Price is Right: Predicting Prices with Product Images." [Online]. Available: www.kaggle.com/jshih7/car-price-prediction

[19] B. Liu *et al.*, "Deep Learning Inversion of Electrical Resistivity Data," pp. 1–14.

[20] A. Akbarimajd *et al.*, "Learning-to-augment incorporated noise-robust deep CNN for detection of COVID-19 in noisy X-ray images," *Journal of Computational Science*, p. 101763, Jul. 2022, doi: 10.1016/j.jocs.2022.101763.

[21] T. Zhang *et al.*, "A neural network architecture optimizer based on DARTS and generative adversarial learning," *Information Sciences*, vol. 581, pp. 448–468, Dec. 2021, doi: 10.1016/j.ins.2021.09.041.

[22] N. Gaggion *et al.*, "ChronoRoot: High-throughput phenotyping by deep segmentation networks reveals novel temporal parameters of plant root system architecture," *Gigascience*, vol. 10, no. 7, Jul. 2021, doi: 10.1093/gigascience/giab052.

[23] L. Dong, F. Jiang, M. Wang, and X. Li, "Fuzzy deep wavelet neural network with hybrid learning algorithm: Application to electrical resistivity imaging inversion," *Knowledge-Based Systems*, vol. 242, p. 108164, 2022, doi: 10.1016/j.knosys.2022.108164.

[24] D. Guo, J. Juan, L. Chang, J. Zhang, and D. Huang, "Discrimination of plant root zone water status in greenhouse production based on phenotyping and machine learning techniques," *Scientific Reports*, vol. 7, no. 1, Dec. 2017, doi: 10.1038/s41598-017-08235-z.

[25] G. Lobet *et al.*, "Using a structural root system model to evaluate and improve the accuracy of root image analysis pipelines," *Frontiers in Plant Science*, vol. 8, Apr. 2017, doi: 10.3389/fpls.2017.00447.

[26] L. Pagès, C. Bécel, H. Boukcim, D. Moreau, C. Nguyen, and A. S. Voisin, "Calibration and evaluation of ArchiSimple, a simple model of root system architecture," *Ecological Modelling*, vol. 290, no. C, pp. 76–84, 2014, doi: 10.1016/j.ecolmodel.2013.11.014.

[27] F. Hochholdinger, C. Marcon, J. A. Baldauf, P. Yu, and F. P. Frey, "Proteomics of Maize Root Development," vol. 9, no. March, pp. 1–7, 2018, doi: 10.3389/fpls.2018.00143.

[28] G. Lobet *et al.*, "Using a structural root system model to evaluate and improve the accuracy of root image analysis pipelines," *Frontiers in Plant Science*, vol. 8, Apr. 2017, doi: 10.3389/fpls.2017.00447.